Effects of genuine dimension-six Higgs operators

Vernon Barger,[1,*] Tao Han,[1,3,†] Paul Langacker,[1,2,‡] Bob McElrath,[1,§] and Peter Zerwas[3,‖]

[1]*Department of Physics, University of Wisconsin, Madison, Wisconsin 53706, USA*
[2]*Department of Physics and Astronomy, University of Pennsylvania, Philadelphia, Pennsylvania 19104, USA*
[3]*Deutsches Elektronen-Synchrotron, D-22603 Hamburg, Germany*
(Received 4 February 2003; published 2 June 2003)

We systematically discuss the consequences of genuine dimension-six Higgs operators. These operators are not subject to stringent constraints from electroweak precision data. However, they can modify the couplings of the Higgs boson to electroweak gauge bosons and, in particular, the Higgs self-interactions. We study the sensitivity to which those couplings can be probed at future e^+e^- linear colliders in the sub-TeV and in the multi-TeV range. We find that for $\sqrt{s} = 500$ GeV with a luminosity of 1 ab^{-1} the anomalous WWH and ZZH couplings may be probed to about the 0.01 level, and the anomalous HHH coupling to about the 0.1 level.

I. INTRODUCTION

Once the Higgs boson is discovered in future collider experiments, the study of its properties will become the next important goal to fully establish the nature of electroweak symmetry breaking [1]. In the standard model (SM), electroweak symmetry breaking is generated by the Higgs potential

$$V_{SM} = \mu^2 |\Phi|^2 + \lambda |\Phi|^4 = \lambda \left(|\Phi|^2 - \frac{v^2}{2} \right)^2 + \text{const} \quad (1)$$

for $\mu^2 < 0$. The parameter $v = \sqrt{-\mu^2/\lambda}$, the vacuum expectation value (VEV) of the Higgs field, is determined experimentally from the well-measured Fermi coupling, $v = 1/\sqrt{\sqrt{2}G_F}$, to be 246 GeV. The Higgs boson mass is predicted by the theory to be $m_H^2 = 2\lambda v^2$. Once the Higgs boson mass is measured, λ is determined and the SM Higgs potential is fully reconstructed. However, new physics beyond the SM is likely to affect the Higgs sector. If there are no light degrees of freedom beyond the Higgs boson that show up in the near future collider experiments, it will be imperative to scrutinize the interactions of the Higgs boson with the electroweak gauge bosons as well as the Higgs self-interactions, to search for evidence of potential extensions of the standard model.

In this report we study the consequences of genuine dimension-six (dim-6) Higgs operators. These operators can be induced by integrating out heavy massive degrees of freedom in a theory beyond the SM, or they may reflect the composite nature of the Higgs boson. Their existence would provide indirect signatures of new physics that couples significantly to the electroweak symmetry breaking sector. Most naturally, they may be interpreted as the first set of operators in a series with rising dimensionality of order $1/\Lambda^{2n}$. There-fore they are expected to be "small" with respect to the SM operators so that the series may be truncated at dim=6 for energies near the electroweak scale in a first approach to the underlying comprehensive theory.

Most dim-6 operators involving the SM fermions and gauge bosons [2,3] are subject to stringent constraints from the current precision data [4,5]. The operators involving the top quark and Higgs field are less severely bounded, but may be constrained by theoretical considerations [6]. Moreover, they will be studied to a good precision at hadron colliders [7] and at future linear colliders [8,9]. Those operators involving no other SM fields but the Higgs fields,

$$\mathcal{O}_1 = \frac{1}{2} \partial_\mu (\Phi^\dagger \Phi) \partial^\mu (\Phi^\dagger \Phi) \quad \text{and} \quad \mathcal{O}_2 = -\frac{1}{3} (\Phi^\dagger \Phi)^3, \quad (2)$$

are much less constrained, and they offer potential sensitivity to genuinely new structures in the Higgs sector. The associated Lagrangian is given by the sum

$$\mathcal{L}' = \sum_i^2 \frac{f_i}{\Lambda^2} \mathcal{O}_i, \quad (3)$$

where Λ is the energy cutoff at which the new physics threshold is open and the effective operator approach ceases to be valid. One naively expects that the scale is near 1 TeV and that the coefficients f_i are order of 1 to 4π. Our convention with the relative negative sign in $\mathcal{O}_2$ reflects that this term is induced in the Higgs potential.

In Sec. II we study the genuine dim-6 Higgs operators of our current interest, involving only the Higgs field, and their effects on the electroweak symmetry breaking. We then present their corrections to the Higgs boson mass and couplings. In Sec. III, we discuss to what extent the couplings may be probed at e^+e^- linear colliders, such as the DESY TeV Energy Superconducting Linear Accelerator (TESLA) [10] and Next Linear Collider (NLC) or Japan Linear Collider (JLC) [11], with both single Higgs boson and Higgs boson pair production at energies $\sqrt{s} = 500$ and 800 GeV. In Sec. IV, we explore the sensitivity at a multi-TeV collider, as envisaged with CERN Linear Collider (CLIC) [12], for 3 and

———————
*Email address: barger@oriole.physics.wisc.edu
†Email address: than@pheno.physics.wisc.edu
‡Email address: pgl@electroweak.hep.upenn.edu
§Email address: mcelrath@pheno.physics.wisc.edu
‖Email address: zerwas@mail.desy.de

5 TeV. We summarize our results in Sec. V. Some details of the analysis for the Higgs sector with dim-6 operators are presented in the Appendix.

II. GENUINE DIMENSION-SIX OPERATORS IN THE HIGGS SECTOR

At the dimension-six level, operators involving four SM light fermions are subject to stringent constraints from the current experimental measurements at low energies [5]. Several operators involving SM gauge bosons and the Higgs field are also constrained from the precision electroweak data and from the triple gauge boson self-interactions [3,4]. The operators involving the top quark and Higgs field seem to be less constrained. However, since they are usually related to anomalous couplings of $Zt\bar{t}$ and $Wt\bar{b}$ by gauge invariance, they will be studied to a high precision when large samples of top quarks are available at hadron colliders [7] and future linear colliders [8,9]. Therefore we will not discuss them further.

There are only two[1] independent operators, $\mathcal{O}_1$ and $\mathcal{O}_2$ defined in Eq. (2), at dimension-six that can be constructed solely from the Higgs field as invariant singlets under all SM gauge transformations and that are free of constraints from existing measurements. In particular, the ρ-parameter will not be affected by these two operators.

Before we study the physical consequences of the operators, it is interesting to relate this set-up of operators to another approach, the Higgs potential expansion. A general Higgs potential with higher dimensional operators can be constructed as [13,14]

$$V_{eff} = \sum_{n=0} \frac{\lambda_n}{\Lambda^{2n}} \left(|\Phi|^2 - \frac{v^2}{2} \right)^{2+n}. \tag{4}$$

This expansion systematically includes all higher order terms in the effective Higgs potential. For instance, at the dim-6 level ($n=1$), the identification between Eqs. (1)–(3) and (4) is

$$\mu^2 = -\left(\lambda_0 - \frac{3\lambda_1 v^2}{4\Lambda^2} \right) v^2, \quad \lambda = \lambda_0 - \frac{3\lambda_1 v^2}{2\Lambda^2}, \quad f_2 = 3\lambda_1. \tag{5}$$

The specific form of Eq. (4) is clearly motivated by the small field expansion of the potential around the vacuum v, which is fixed at any given order with $V_{eff}=0$. On the other hand, the general dim-6 expansion in Eq. (3) includes derivative

---

[1] The operator $\mathcal{O}_3 = (D_\mu \Phi)^\dagger \Phi \Phi^\dagger D^\mu \Phi$ affects the two-point functions of the W,Z gauge bosons and thus contributes to the ρ parameter, leading to $\rho = 1 - f_3 v^2/2\Lambda^2$. The current constraint from the precision electroweak data [5] yields a 95% C.L. bound $|f_3|v^2/2\Lambda^2 < 0.0050$ for $f_3 < 0$ and < 0.0011 for $f_3 > 0$. This implies that $-0.17 < f_3 \leq 0$ or $0 \leq f_3 < 0.036$ if $\Lambda = 1$ TeV. Such a small coefficient will not result in significant corrections to the SM Higgs sector. We therefore ignore $\mathcal{O}_3$ in our further analysis and focus on the other two operators.

operators that lead to corrections to the kinetic terms and the Higgs-field derivative couplings.

Higher dimensional operators can arise from integrating out heavy massive degrees of freedom in theories beyond the SM, or via radiative corrections. In weakly coupled theories such as supersymmetry, the effects are typically small before reaching the new physics threshold. The contribution is usually loop-induced and it is suppressed by a factor of $1/16\pi^2$. However, if new strong dynamics is involved in the electroweak sector [15], the effects could be quite appreciable. In particular, the Higgs self-interactions parameterized by the dim-6 operators may be significant [16]. The effects of these operators on the triviality and stability of the theory were studied in [17].

A. Electroweak symmetry breaking

In the presence of dim-6 operators, the modified effective Higgs potential may be written as

$$V_{eff} = \mu^2 |\Phi|^2 + \lambda |\Phi|^4 + \frac{f_2}{3\Lambda^2} |\Phi|^6. \tag{6}$$

Electroweak symmetry breaking is obtained via a non-zero vacuum expectation value of the scalar field. Minimizing the potential of Eq. (6) with respect to $|\Phi|^2$ leads to the following expression for the ground state of the field:

$$\langle |\Phi|^2 \rangle \equiv \frac{v^2}{2} = \frac{\Lambda^2}{f_2} (-\lambda \pm \sqrt{\lambda^2 - f_2 \mu^2/\Lambda^2}). \tag{7}$$

Interpreting the dim-6 operators as small corrections in the vicinity of the local minimum of the Higgs potential, the new term in Eq. (6) should be bounded by

$$\frac{|f_2 \mu^2|}{\lambda^2 \Lambda^2} \ll 1 \quad \text{or} \quad \frac{|f_2|}{|\lambda|} \frac{v_0^2}{\Lambda^2} \ll 1, \tag{8}$$

where $v_0^2 \equiv |\mu^2/\lambda|$ is the standard VEV of the Higgs field in the SM limit. At the same time the signs of the bilinear coupling $\mu^2 < 0$ and the quartic coupling $\lambda > 0$ must be fixed such that the standard model is reproduced for large Λ^2. Moreover, the sign in the solution (7) must be chosen positive for the solution close to the standard model. f_2 may acquire either sign. (Alternative assignments and their consequences are discussed in the Appendix.) Expanding the solution in $1/\Lambda^2$, we find for the ground state of the Higgs field:

$$\frac{v^2}{2} \approx \frac{v_0^2}{2} \left(1 - \frac{f_2 v_0^2}{4\lambda \Lambda^2} \right) \tag{9}$$

where we have rewritten the expression in terms of the minimal SM VEV v_0^2. Thus the dim-6 addition to the Higgs potential leads to a small shift of the Higgs field in the vacuum, decreasing or increasing its strength depending on whether the dim-6 part of the potential is repulsive or attractive. The value of v is determined by the Fermi coupling G_F as noted earlier.

B. Corrections to Higgs boson couplings

We first note that the dim-6 operator $\mathcal{O}_1$ affects the kinetic terms of the Higgs boson propagation; see Eqs. (A3) and (A17). Thus we must re-scale the field ϕ to define the canonically normalized Higgs field H

$$\phi = NH, \quad \text{with} \quad N = \left(1 + \frac{f_1 v^2}{\Lambda^2}\right)^{-1/2} \approx 1 - \frac{1}{2} a_1, \quad (10)$$

where

$$a_1 = \frac{f_1 v^2}{\Lambda^2}. \quad (11)$$

With this field redefinition, we find for the physical Higgs boson mass

$$m_H^2 \approx 2\lambda v^2 \left(1 - \frac{f_1 v^2}{\Lambda^2} + \frac{f_2 v^2}{2\lambda \Lambda^2}\right) = 2\lambda v^2 \left(1 - a_1 + \frac{a_2}{2\lambda}\right), \quad (12)$$

where

$$a_2 = \frac{f_2 v^2}{\Lambda^2}. \quad (13)$$

Equation (12) implies that the Higgs boson mass m_H and the Higgs self-coupling λ are in general independent parameters when new physics beyond the SM is taken into account. The mass does not only depend on the quartic coupling but also on the small but otherwise arbitrary dim-6 couplings of the generalized potential. Since the Higgs boson mass will be directly measured with very high precision, it is more natural to express all observables in terms of m_H instead of λ, as we will do for the rest of the paper.

For the Higgs couplings to the SM particles, the Higgs field is renormalized by the factor N, which results in the interactions

$$\mathcal{L}_M = \left(M_W^2 W_\mu^+ W^{-\mu} + \frac{1}{2} M_Z^2 Z_\mu Z^\mu\right)\left(\left(1 - \frac{a_1}{2}\right)\frac{2H}{v}\right.$$
$$\left. + (1 - a_1)\frac{H^2}{v^2}\right). \quad (14)$$

The Higgs self-interactions can similarly be expressed in terms of v, m_H and the anomalous couplings a_1, a_2,

$$\mathcal{L}_{H^3} = -\frac{m_H^2}{2v}\left(\left(1 - \frac{a_1}{2} + \frac{2a_2}{3}\frac{v^2}{m_H^2}\right)H^3 - \frac{2a_1 H \partial_\mu H \partial^\mu H}{m_H^2}\right) \quad (15)$$

$$\mathcal{L}_{H^4} = -\frac{m_H^2}{8v^2}\left(\left(1 - a_1 + \frac{4a_2 v^2}{m_H^2}\right)H^4 - \frac{4a_1 H^2 \partial_\mu H \partial^\mu H}{m_H^2}\right). \quad (16)$$

The $\mathcal{O}_1$ operator, beyond changing the strength of the self-interactions, introduces derivative couplings of the Higgs field. They grow with energy and thus will be more significant in a multi-TeV collider. The $\mathcal{O}_2$ operator, however, affects only the strength of the standard triple and quartic Higgs boson self-interactions. Some details are given in the Appendix.

C. Experimental probe of the anomalous couplings

Unlike many studies in the literature which discuss the achievable accuracies to determine the Higgs couplings in the SM, we stress that our treatment is a consistent approach to systematically include new physics effects in the Higgs sector beyond the SM up to the order of $1/\Lambda^2$. In addition to the Higgs boson mass, we have introduced two new parameters, $a_i = f_i v^2/\Lambda^2$ ($i = 1,2$), referred to as *Higgs anomalous couplings*, each of which in turn is related to a model parameter f_i and the new physics cutoff scale Λ. If we naively set the cutoff scale to a value of 1 TeV, we have $a_i \approx f_i/16$. In the rest of the paper, we explore the range of parameters

$$-0.5 < a_1, \quad a_2 < 0.5, \quad (17)$$

which allows f_i to be about 4π or less.

The expected Higgs signal cross section depends upon the anomalous couplings. Assuming the signal cross section can be factorized as a product of the SM cross section and a factor depending on the anomalous couplings,

$$\sigma = F(a_i)\sigma_{SM}, \quad (18)$$

we can relate the accuracy of the cross section measurements to the change of the anomalous couplings

$$\Delta\sigma = \frac{\partial\sigma}{\partial a_i}\Delta a_i, \quad \frac{\Delta\sigma}{\sigma} = \frac{\partial F}{\partial a_i}\frac{\Delta a_i}{F}. \quad (19)$$

We identify the relative error on the signal cross section measurement as the statistical uncertainty of the experiment

$$\frac{\Delta\sigma}{\sigma} = \sqrt{\frac{S+B}{S}}, \quad (20)$$

where $S = L\sigma = F(a_i)S_{SM}$ is the expected signal events with an integrated luminosity L, B is the (non-Higgs) background. We thus determine the error on the anomalous coupling in terms of SM quantities and the function $F(a_i)$

$$\Delta a_i = \left(\frac{\partial F}{\partial a_i}\right)^{-1}\frac{\sqrt{FS_{SM}/B+1}}{S_{SM}/\sqrt{B}} \approx \left(\frac{\partial F}{\partial a_i}\right)^{-1}\sqrt{\frac{F}{S_{SM}}}, \quad (21)$$

where the last approximation is for zero background B. The above estimate is based on simple Gaussian statistics, so the event sample should be sizable, typically $S \gtrsim 10$ or so. Also note that a realistic event determination should include the branching fraction and experimental efficiency factors for a specific channel, which should be folded in to S and B here.

Another advantage of our treatment is the factorized formulation as in Eqs. (18) and (21). Once the new physics contribution is formulated as F, the sensitivity studies will depend only upon the SM calculations. In other words, real-
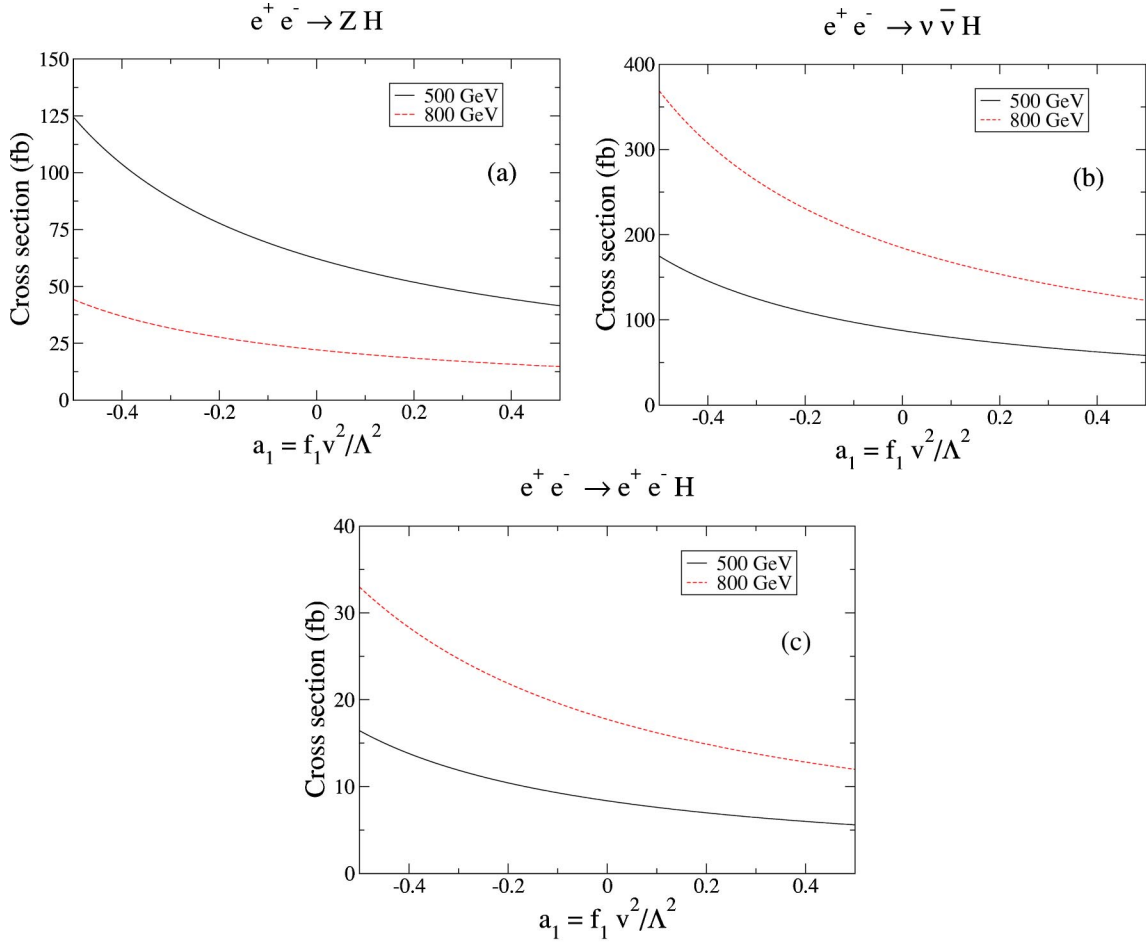
$$e^+ e^- \to Z H$$

(a)

$$e^+ e^- \to \nu \bar{\nu} H$$

(b)

$$e^+ e^- \to e^+ e^- H$$

(c)

FIG. 1. Cross sections for single Higgs boson production versus a_1 at $\sqrt{s} = 500$ and 800 GeV for (a) Higgs-strahlung, (b) *WW*-fusion, and (c) *ZZ*-fusion, with $m_H = 120$ GeV.

istic SM signal or background simulations [10,18–20] may then be transformed into a measurement of a_i by Eq. (21).

III. ANOMALOUS HIGGS BOSON COUPLINGS AT LINEAR COLLIDERS

A. Single Higgs production with anomalous couplings

The processes of single Higgs production include

$$e^+ e^- \to ZH, \qquad (22)$$

$$e^+ e^- \to \nu \bar{\nu} H \quad \text{and} \quad e^+ e^- H. \qquad (23)$$

The Higgs-strahlung process (ZH) dominates for moderate values of the Higgs boson mass near the production threshold $\sqrt{s} \sim M_Z + m_H$, but falls like $1/s$ at higher energies. The *WW* and *ZZ*-fusion processes of Eq. (23) take over at higher energies due to the logarithmic enhancement $\ln^2(s/M_W^2) \times \ln(s/m_H^2)$; the clean channel $e^+ e^- H$ via *ZZ*-fusion allows the complete reconstruction of the final state but the cross section is smaller than that from *WW* fusion by about an order of magnitude due to the weak electron neutral-current coupling. In our treatment, we have separated the weak bo-

son fusion processes from those involving the resonant Z decay to $e^+ e^-$ or $\nu \bar{\nu}$. This can be achieved by appropriate kinematic cuts [21].

At tree level each diagram in these processes involves exactly one Higgs vertex, and thus the field redefinition N can be factored out of the cross section, cf. [22], giving a simple tree level relation for any single Higgs production process:

$$\sigma = N^2 \sigma_{SM} = \frac{\sigma_{SM}}{1 + a_1}. \qquad (24)$$

We present the total cross sections[2] of single Higgs boson production in Fig. 1 for $\sqrt{s} = 500$, 800 GeV and $m_H = 120$ GeV versus a_1. All of the plots display similar behavior. For negative values of a_1 the cross section increases and for positive values of a_1 the cross section decreases while results at $a_1 = 0$ correspond to the SM prediction.

We combine four final state channels:

---

[2] The evaluation of the diagrams has been performed by means of COMPHEP [23].

Higgs-strahlung where $Z \to \ell^+ \ell^-$ ($\ell = e$ or μ) and Higgs boson decays into anything;

Higgs-strahlung where $Z \to \nu \bar{\nu}$ and $H \to b \bar{b}$;

ZZ-fusion where Higgs boson decays into anything;

WW-fusion where $H \to b \bar{b}$.

These four channels belong to two well-studied event topologies: $\ell^+ \ell^-$ to reconstruct m_H via the recoil mass while H can decay into anything; $H \to b \bar{b}$ plus large missing energy due to the neutrinos. For the lepton pair final state, we adopt the acceptance cuts to identify the Higgs signal

$$p_T(\ell) > 15 \text{ GeV}, \quad |\cos \theta_\ell| < 0.8, \quad M_{recoil} > 70 \text{ GeV}. \tag{25}$$

We also impose additional cuts to further remove the backgrounds, for the Higgs-strahlung

$$p_T(\ell\ell) > 80 \text{ GeV}, \quad |M_Z - m(\ell\ell)| < 10 \text{ GeV}, \tag{26}$$

and for the ZZ fusion

$$m(\ell\ell) > 100 \text{ GeV}. \tag{27}$$

As for $H \to b \bar{b}$ plus missing neutrinos, we demand 2-b tag and select events with

$$p_T(b) > 20 \text{ GeV}, \quad |\cos \theta_b| < 0.8,$$

$$M_{missing} > 70 \text{ GeV}, \quad |m_H - m(bb)| < 10 \text{ GeV}. \tag{28}$$

All of the cuts preserve the signal rate for about 80% efficiencies. Identification efficiencies of 80% for b-tagging and 99% for each lepton are included [10]. Although the $\ell^+ \ell^-$ final state can reconstruct the Higgs signal very nicely, the $H \to b \bar{b}$ from WW-fusion and $Z \to \nu \bar{\nu}$ yields a larger rate and turns out to be more helpful for the coupling determination.

Given the experimentally observed number of events S, along with the expected SM prediction for the Higgs events S_{SM} and for the (non-Higgs) background events B, the value of a_1 and its statistical error on it can be estimated via Eq. (21). We combine the channels of different topology by quadrature to obtain the total error

$$\frac{1}{\Delta a_2} = \left(\sum_j \frac{1}{\Delta a_{2_j}^2} \right)^{1/2}. \tag{29}$$

Since the Higgs signal identification by the mass reconstruction in these channels can be highly efficient at a linear collider, the backgrounds are smaller than the signal rates after the stringent cuts. We thus take the zero-background approximation. Assuming an integrated luminosity of 1 ab^{-1}, we plot the combined statistical accuracy on measuring a_1 in Fig. 2. We find impressive high sensitivity to those Higgs production processes. For instance, for $a_1 = 0$, $\Delta a_1 \approx 0.005$ from Fig. 2, which corresponds to an SM coupling measurement about 0.5%. For non-zero values of a_1, we may reach a typical sensitivity like $a_1 \approx 0.5 \pm 0.01$. If we had included the backgrounds in the analysis, our results on the sensitivity
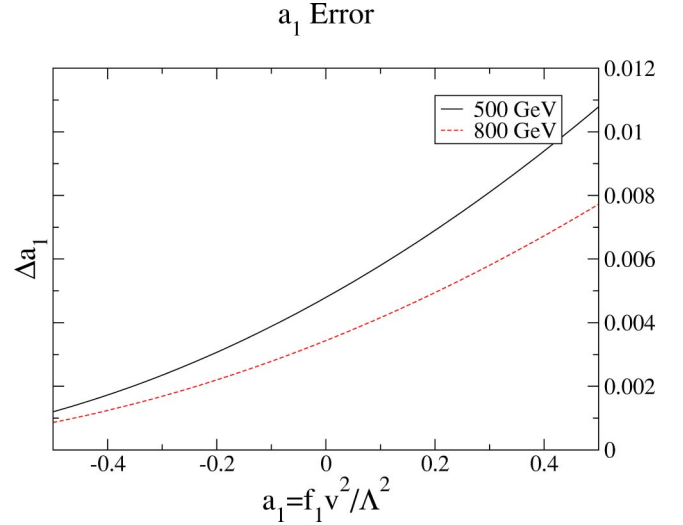

FIG. 2. Combined statistical accuracy on a_1 with an integrated luminosity of 1 ab^{-1} for $\sqrt{s} = 500$ GeV and 800 GeV, using the Higgs-strahlung, the WW-fusion and ZZ-fusion channels, as described in the text; $m_H = 120$ GeV.

would not change by more than a factor of $\sqrt{2}$. These estimates are close to the results obtained from detailed experimental simulations, cf. Ref. [10]. Further improved analysis can be converted into an expected measurement of a_1 using Eqs. (24) and (21).

Similar results are expected also for larger Higgs boson masses. For example, the cross section (and therefore the anomalous coupling a_1) for Higgs-strahlung at a 500 GeV collider with $m_H = 240$ GeV can be measured with an accuracy of 4% [24], corresponding to a measurement of the ZZH coupling to 2%. The measurement of a_1 can be improved later with increasing statistics for W-boson fusion at a high-luminosity TeV collider.

The energy scale for new physics or composite structure in the Higgs sector may be inferred from

$$\Lambda = \sqrt{\frac{f_i}{a_i}} v. \tag{30}$$

For a representative coupling $f_1 \approx 1$ and an accuracy $a_1 < 0.005$, the resulting energy scale can therefore be bounded to $\Lambda \gtrsim 3.5$ TeV. Thus, these experiments will probe the entire threshold region of potentially new strong interactions generating the mechanism for electroweak symmetry breaking.

B. Double Higgs production with anomalous couplings

The production of two Higgs particles may allow us to probe the anomalous couplings in $WWHH$, $ZZHH$, HHH, where the triple Higgs vertex involves the new operator $\mathcal{O}_2$ which appears to be rather secluded from commonly accessible processes. The dominant processes that involve these couplings at linear colliders are [25,26]
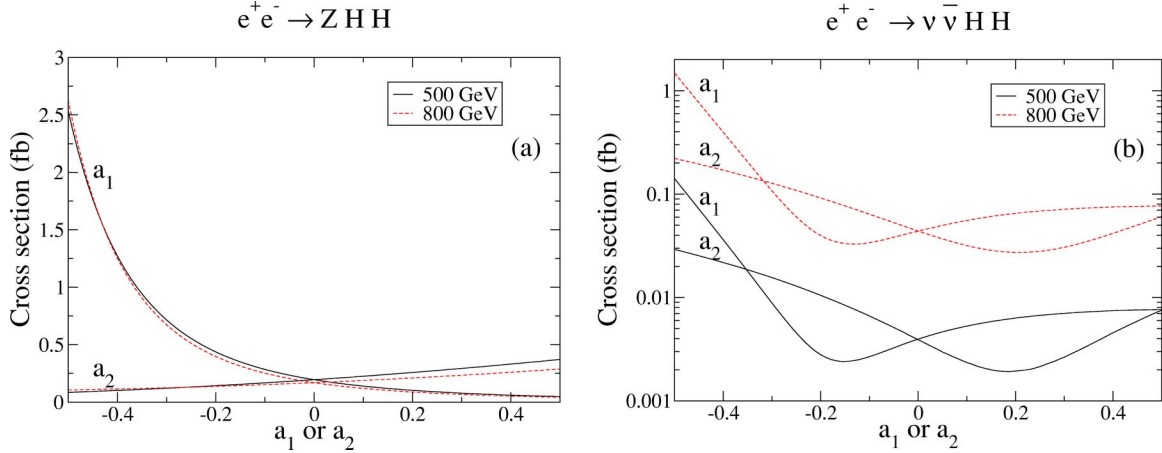
$$e^+ e^- \to ZHH, \tag{31}$$

FIG. 3. Cross sections for double Higgs production at $\sqrt{s}=500$ and 800 GeV versus a_1 and a_2 by (a) Higgs-strahlung, (b) *WW*-fusion, with $m_H=120$ GeV.

$$e^+e^- \to \nu\bar{\nu}HH. \tag{32}$$

The process $e^+e^- \to e^+e^-HH$ via *ZZ*-fusion again is smaller than the *WW*-fusion by about an order of magnitude, and thus is not considered here. The accuracy of measuring the SM coupling g_{HHH} has recently been studied at the LC in Ref. [19,22,27,28], and at CLIC in Ref. [20]. Extensions to supersymmetric Higgs pair production [26] and to two-Higgs doublet models [29] have also been explored in detail.

Inspecting the increasing order of the electroweak couplings and the increasing number of heavy particles in the final states for the diagrams of single Higgs-strahlung and double Higgs-strahlung, it is clear that single Higgs-strahlung will provide the far better bound or measurement of the anomalous coupling a_1. This parameter is therefore taken as a fixed input, $a_1=0$ for definiteness, for bounding or measuring the new parameter a_2 in double Higgs-strahlung.

The total cross sections versus a_2 at $\sqrt{s}=500$ and 800 GeV are presented in Fig. 3 for the double-Higgs-strahlung and *WW*-fusion. For completeness the dependence on a_1 is also shown in the figures. The contribution from an anomalous triple Higgs coupling that is derivatively coupled, is essentially proportional to a_1. It becomes increasingly important only at higher energies.

The only contribution from a_2 comes from the triple Higgs self-interaction. These cross sections are formally quadratic as a function of a_2, resulting from the triple Higgs coupling being linear in a_2. The minimum of the cross section in a_2 moves with energy, and its location in a_2 is determined by the size of the crossing of the triple-Higgs diagram with the other diagrams and itself. For instance, in Fig. 3(a) of the *ZHH* plot at 500 GeV the minimum occurs at $a_2 \simeq -2.4$.

With our parametrization of the anomalous couplings, the cross section is quadratic in a_2. We can thus factor out the a_2 dependence of the cross section

$$\frac{\sigma(a_2)}{\sigma_{SM}} = F(a_2) = A a_2^2 + B a_2 + C, \tag{33}$$

with the normalization $C=1$. The other coefficients A,B are fitted to the full calculations and are given in Table I. For the *ZHH* production, the linear term clearly dominates. For the *WW*-fusion process, the linear term is more important for $a_2 < 0.4$.

The error on the measurement of a_2 is determined by Eq. (21). The event analysis is similar to that in Sec. III A, except that we require at least 3-*b* tagging and construct both Higgs mass peaks. We combine the errors from the *ZHH* and *WW*-fusion channels in quadrature as in Eq. (29). The statistical accuracy is presented in Fig. 4. We see that for $a_2=0$, we have $\Delta a_2 \approx 0.1$. For non-zero values of a_2, we may reach a typical sensitivity like $a_2 \approx 0.5 \pm 0.1$. The worst sensitivity comes near $a_2 \approx 0.2$, where the cross sections reach minimum, see Fig. 3(b).

Since there are a number of studies on the triple Higgs coupling, we can convert the usual $\delta g_{HHH}/g_{HHH}$ to our Δa_2 at $a_2=0$ and compare with our results. From Eq. (15), we have, for $m_H=120$ GeV and $a_2=0$,

$$\frac{\delta g_{HHH}}{g_{HHH}} = \frac{2v^2 \delta a_2}{3m_H^2 + 2v^2 a_2} \approx 2.8 \Delta a_2. \tag{34}$$

Using the results of Ref. [19] on $\delta g_{HHH}/g_{HHH}$ at 500 GeV, we obtain the estimated accuracy on Δa_2

TABLE I. Parameters A,B as in Eq. (33).

Process	$\sqrt{s}$	A	B
	500 GeV	0.675	1.47
	800 GeV	0.657	1.08
ZHH	3 TeV	0.374	0.346
	5 TeV	0.264	0.243
	500 GeV	14.8	−5.51
	800 GeV	8.84	−3.66
$\nu\bar{\nu}HH$	3 TeV	3.21	−1.69
	5 TeV	2.42	−1.34

a_2 Error
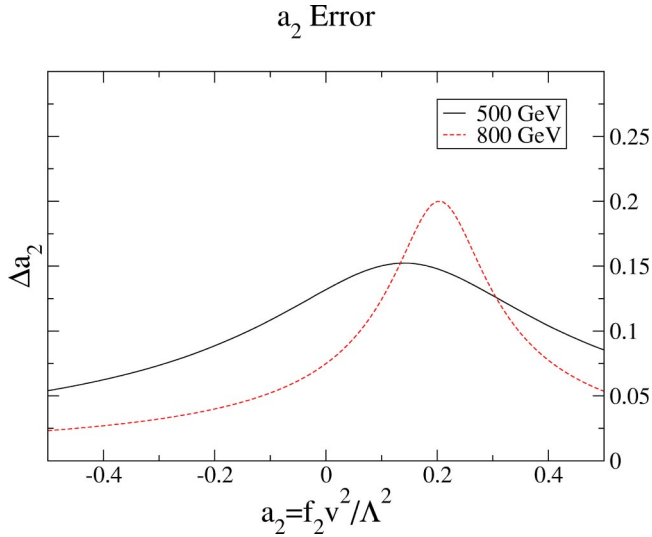

FIG. 4. Combined statistical accuracy on a_2 with an integrated luminosity of 1 ab^{-1} for $\sqrt{s} = 500$ GeV and 800 GeV, using the Higgs-strahlung and the WW-fusion channels, as described in the text; $m_H = 120$ GeV.

Luminosity	500 fb^{-1}	1 ab^{-1}	2 ab^{-1}
$\delta g_{HHH}/g_{HHH}$	42%	30%	20%
Δa_2	0.15	0.11	0.073

This is consistent with our results for $a_2 = 0$ given in Fig. 4. Note that for $a_2 \lesssim 0.073$, the bound corresponds to an energy scale of $\Lambda \gtrsim 910$ GeV, assuming $f_1 = 1$ and $m_H = 120$ GeV.

For a heavier Higgs boson, higher collider energies are needed to provide enough phase space for the production of several heavy particles in the final state. While the accuracies for the HHH coupling and the anomalous coupling a_2 at 800 GeV can only be expected [26] of order unity for $m_H = 180$ GeV, they improve to 11.5% for g_{HHH} and to 9.2% for a_2 at a 3 TeV collider after collecting a luminosity of 3 ab^{-1} [30] (see next section).

IV. ANOMALOUS HIGGS BOSON COUPLINGS AT CLIC

At higher energy colliders such as CLIC [31] with c.m. energies of $\sqrt{s} = 3$ to 5 TeV, it is quite possible that new physics thresholds may open and new massive particles be produced. In the pessimistic scenario that there are no new particles produced, higher energy colliders will probe new physics phenomena indirectly at a higher energy scale $\Lambda \gtrsim \sqrt{s}$. In particular, energy-dependent operators will have significant enhancements, while the s-channel SM processes will be suppressed at higher energies.

A. Higgs production with anomalous couplings

We first show the total cross sections for single and double Higgs production at the proposed CLIC energies versus the anomalous couplings a_1 and a_2 in Fig. 5, where we have only included the dominant channels via WW and ZZ fusion. It is obvious that due to the much larger production rate, a_1 can be probed better via the single Higgs production processes. For Higgs pair production, the processes are again more sensitive to a_2 than a_1. The statistical accuracy on a_1 can be estimated similarly to the case of low energies. We adopt the same cuts as in Sec. III A. We see from Fig. 6 that the statistical sensitivity of probing a_1 and a_2 at CLIC is improved by roughly a factor of two to three over an LC. However, part of the improvement will be lost as a result of increased experimental complexity owing to the rapidly rising beamstrahlung.

B. The triple-Higgs derivative coupling

The increasing fusion cross sections for single Higgs production with rising energy, cf. Fig. 5, may balance to some extent the loss of clarity in a final state involving neutrinos. The new point at rising energy however will be to probe the derivative contribution to the anomalous tri-linear coupling. The relative size of the corresponding part in the cross section grows quadratically in the energy $\sim E_H^2/m_H^2$. The size of the effect is governed by the parameter a_1 which can be determined from the measurements of single Higgs-strahlung at JLC, NLC, or TESLA. The effect is shown in Fig. 7 in which (a) the cross section difference and (b) the cross section ratio for the double Higgs production in WW-fusion are presented as a function of the collider energy varied between 350 GeV and 5 TeV for a Higgs boson mass $m_H = 120$ GeV. The prediction of the Standard Model is compared with the anomalous contributions for four values of the parameter $a_1 = \pm 0.05, \pm 0.1$. We see from Fig. 7 that the dependence of the cross section on energy with the anomalous coupling a_1 is clearly stronger than that of the SM. However, as observed from the cross section ratio in Fig. 7(b), the energy dependence is rather mild unless a_1 is as large as $a_1 \sim 0.1$, and becomes more appreciable at the CLIC energies $\sqrt{s} \sim 3$ TeV. This is primarily due to the dominant contributions where both Higgs bosons are radiated off W's, that consequently dilute the effect of the energy dependent contribution from the Higgs derivative operators.

V. CONCLUSIONS

If the standard model is embedded as a low energy effective approach in a more comprehensive theory, it is natural to include dimension-six operators as a first step in a systematic operator expansion for parametrizing the physics beyond the standard model. We have discussed in this report the physics consequences of genuine dim-6 operators in the Higgs sector. The operators [with coefficients a_1, a_2 of order v^2/Λ^2] are not subject to stringent constraints from electroweak precision data. These operators renormalize the Higgs kinetic propagation and the Higgs boson mass parameter. Depending on the range of validity for the expansion, they may even affect the vacuum stability of the theory. Moreover, they can modify the couplings of the Higgs boson to gauge bosons and the Higgs self-interactions.

We have studied the sensitivity to which those couplings can be probed at future e^+e^- linear colliders with $\sqrt{s} = 500, 800$ GeV, and in a subsequent second phase, with 3
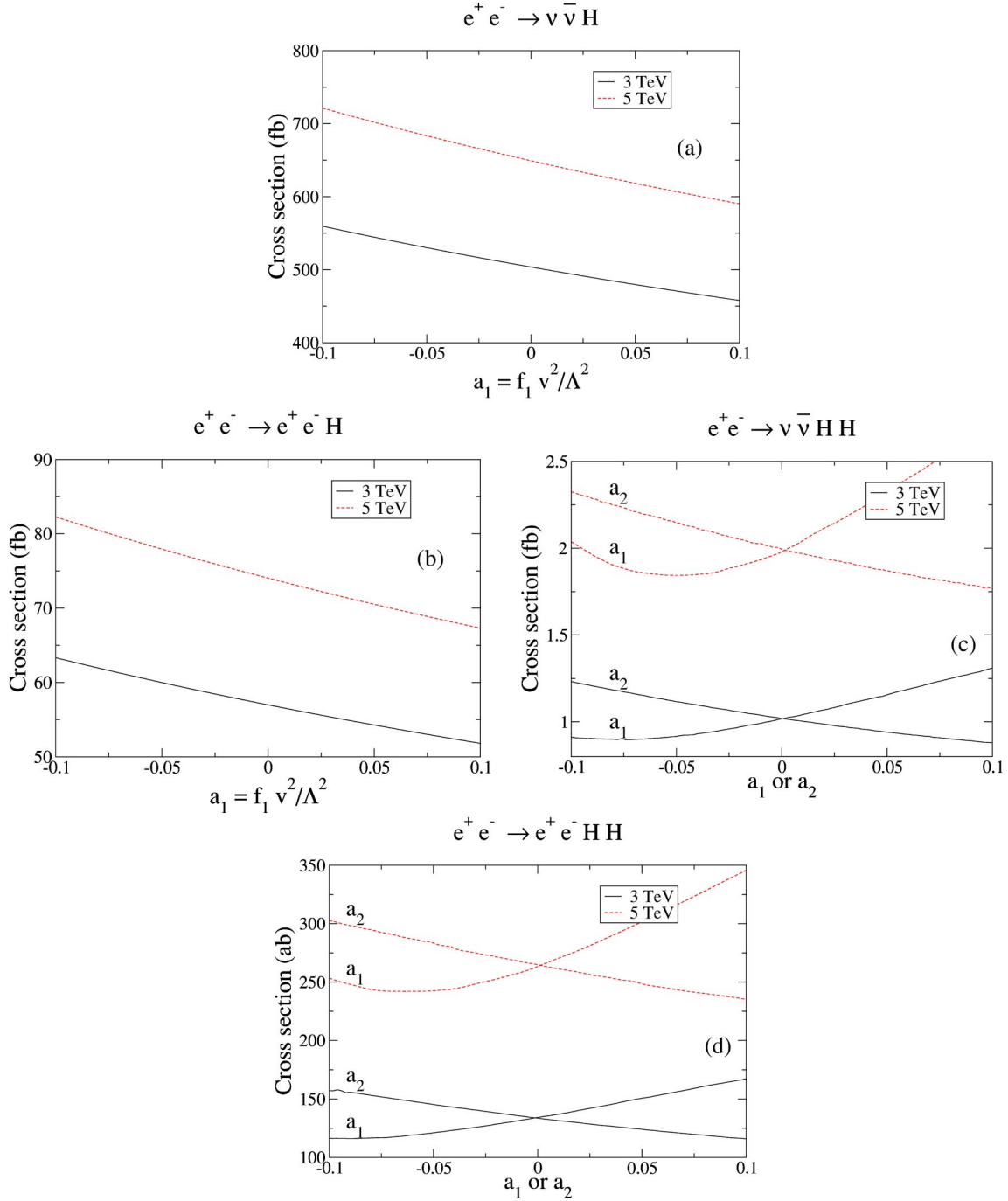
$$e^+ e^- \rightarrow \nu \bar{\nu} H$$

$$e^+ e^- \rightarrow e^+ e^- H \qquad\qquad e^+ e^- \rightarrow \nu \bar{\nu} H H$$

$$e^+ e^- \rightarrow e^+ e^- H H$$

FIG. 5. Cross sections at $\sqrt{s} = 3$ and 5 TeV (a) for single Higgs boson production versus a_1 via *WW*-fusion and (b) via *ZZ*-fusion; (c) for double Higgs boson production versus $a_{1,2}$ via *WW*-fusion and (d) via *ZZ*-fusion, with $m_H = 120$ GeV.

and 5 TeV. We have found good accuracy in probing a_1 and a_2, as presented in Figs. 2 and 4. Some typical values of the accuracy achievable at various collider energies are listed in Table II, both in terms of Δa_i and Λ, presenting the bounds to which dim-6 induced deviations from the SM ($a_i = 0$) can be probed. The coefficient a_1 can be probed, and measured for non-zero values, typically to better than the 0.01 level, and a_2 to the 0.1 level. We recall that $a_i \approx 0.05$, 0.002 for $f_i = 1$ leads to $\Lambda \approx 1$, 5.5 TeV. Thus the sensitivity reachable

at future linear colliders may be sufficient to explore the new effects as parametrized by the dim-6 operators, at energy scales throughout the threshold region of new strong interactions $\lesssim 4\pi v \sim 3$ TeV.

As a final remark in regard of a comparison with hadron colliders: The LC precision tests for Higgs self-couplings are significantly superior to the CERN Large Hadron Collider (LHC) tests. There is little chance to observe at the LHC the Higgs-pair events for a light Higgs boson with m_H
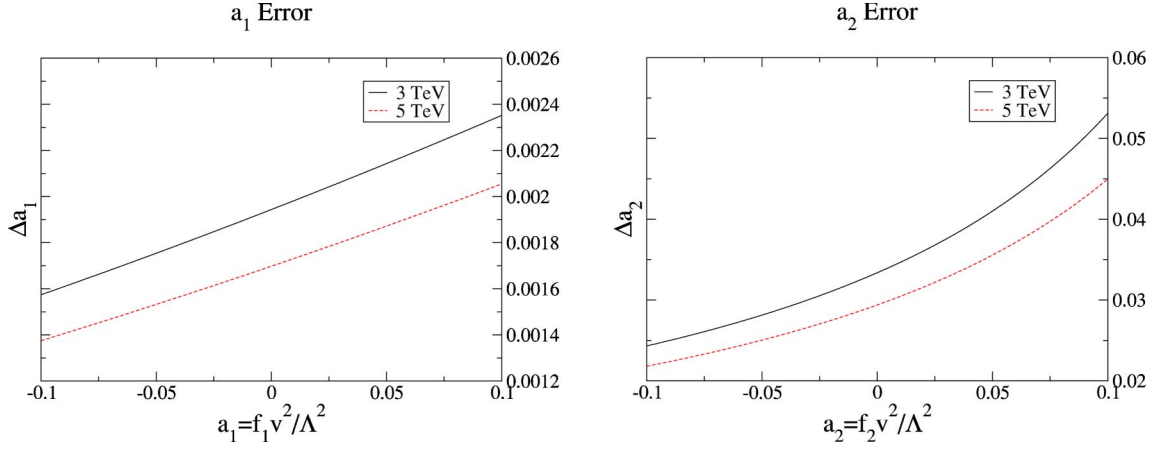
FIG. 6. Combined statistical accuracy on (a) a_1 and (b) a_2 with an integrated luminosity of 1 ab^{-1} for $\sqrt{s}=3$ and 5 TeV, using the WW- and ZZ-fusion channels, as described in the text; $m_H=120$ GeV.

<140 GeV, which dominantly decays to $b\bar{b}$. Only for a heavier Higgs boson in the decay mode $H\rightarrow WW^*$ with leptons in the final state, could the LHC, and thereafter improved by the Very Large Hadron Collider (VLHC), allow a first glimpse [32] of the triple Higgs coupling.

APPENDIX: THE SM HIGGS SECTOR WITH DIMENSION-SIX OPERATORS

In this appendix, we present some details of the effects of the genuine dimension-six Higgs operators in extensions of the standard model. These operators are non-renormalizable and can be induced by integrating out heavy massive degrees of freedom in a more complete theory, as commented in the text.

1. The Higgs sector with genuine dimension-six operators

The SM Lagrangian of the Higgs sector is of the form

$$\mathcal{L}_{SM}=|D_\mu\Phi|^2-V_{SM}, \quad V_{SM}=\mu^2|\Phi|^2+\lambda|\Phi|^4, \quad \text{(A1)}$$

where Φ is the Higgs doublet under the $SU_L(2)$ gauge group. To generate a local minimum away from zero field strength, μ^2 must be chosen negative, while λ must be positive to guarantee the stability of the system. For simplicity we work in the unitary gauge. After shifting the neutral scalar field with respect to its vacuum expectation value to the physical Higgs field H, we write

$$\Phi=\begin{pmatrix}0\\(H+v)/\sqrt{2}\end{pmatrix}, \quad \text{(A2)}$$

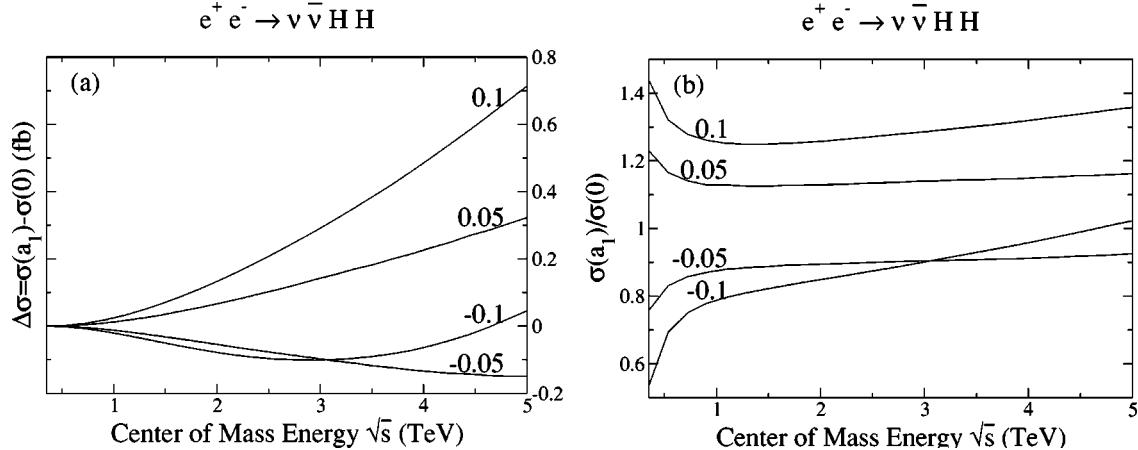where $v=\sqrt{-\mu^2/\lambda}$ is determined by minimizing V_{SM}.

FIG. 7. (a) Cross section difference and (b) ratio to the standard model cross section for double-Higgs production versus energy with $m_H=120$ GeV in WW-fusion for representative values $a_1=-0.1, -0.05, 0.05, 0.1$.

TABLE II. Typical sensitivity Δa_i to be reached as deviations from the SM and the corresponding scales Λ for $f_i=1$ at future linear colliders with 1 ab^{-1}.

	$\sqrt{s}$	Δa_1 (Λ TeV)	Δa_2 (Λ TeV)
	500 GeV	0.0047 (3.6)	0.13 (0.68)
	800 GeV	0.0034 (4.2)	0.075 (0.89)
$m_H = 120$ GeV	3 TeV	0.0020 (5.5)	0.033 (1.4)
	5 TeV	0.0017 (6.0)	0.029 (1.4)

At the dimension-six level, there are only two independent operators that can be constructed purely from the Higgs field and that are not constrained by existing data, as given in Eq. (2). These two operators generate kinetic and mass terms as well as three- and four-point interactions:

$$\mathcal{O}_1 = \frac{1}{2}\partial_\mu H \partial^\mu H (v^2 + 2vH + H^2), \qquad (A3)$$

$$\mathcal{O}_2 = -\frac{1}{24}(15v^4H^2 + 20v^3H^3 + 15v^2H^4). \qquad (A4)$$

The effective Higgs potential is the sum of V_{SM} plus the $\mathcal{O}_2$ term,

$$V_{eff} = \mu^2|\Phi|^2 + \lambda|\Phi|^4 + \frac{f_2}{3\Lambda^2}|\Phi|^6. \qquad (A5)$$

This specific form may be interpreted as an expansion in Φ, truncated after the first anomalous term beyond the basic contributions in the standard model.

2. Electroweak symmetry breaking

The electroweak symmetry breaking is induced by the non-zero vacuum expectation value (VEV) of the scalar field. For curiosity we will ignore the limited range of the truncated series and explore the sexto-linear term in full generality. Conclusions restricted to the "small field" expansion have been elaborated in the main part of the text.

Minimizing the potential Eq. (A5) with respect to $|\Phi|^2$ leads to the VEV

$$\langle|\Phi|^2\rangle \equiv \frac{v^2}{2} = \frac{-\lambda \pm \sqrt{\lambda^2 - f_2\mu^2/\Lambda^2}}{f_2/\Lambda^2} \xrightarrow{\Lambda \gg \mu} (\pm|\lambda| - \lambda)\frac{\Lambda^2}{f_2}$$

$$= \mp\frac{\mu^2}{2|\lambda|} \mp \frac{f_2\mu^4}{8|\lambda|^3\Lambda^2} \pm \mathcal{O}\left(\frac{1}{\Lambda^4}\right). \qquad (A6)$$

To obtain a real solution, a necessary condition is $\lambda^2\Lambda^2 \geq f_2\mu^2$.

There are eight combinations of the sign choices for the three parameters μ^2, λ and f_2. Four of them,

$\mu^2>0, \quad \lambda>0, \quad f_2>0$:   symmetric minimum at $\Phi=0$,

$\mu^2>0, \quad \lambda>0, \quad f_2<0$:   symmetric minimum at $\Phi=0$ and global maximum

$\mu^2>0, \quad \lambda<0, \quad f_2<0$:   symmetric minimum at $\Phi=0$ and global maximum

$\mu^2<0, \quad \lambda<0, \quad f_2<0$:   no minimum

would not give a correct pattern for electroweak symmetry breaking, cf. Fig. 8. We therefore discuss the other four configurations which can give rise to spontaneous symmetry breaking indeed, cf. Fig. 9.

(1) $\mu^2<0$, $\lambda>0$, $f_2>0$. The solution as given in Eq. (A6) is

$$\frac{v^2}{2} = \frac{\lambda\Lambda^2}{f_2}\left(\sqrt{1 + \frac{f_2|\mu^2|}{\lambda^2\Lambda^2}} - 1\right). \qquad (A7)$$

It is easy to check that $V_{eff}(v^2/2)<0$ and that this is a global minimum. Only far away from the standard model [realized for $\Lambda \gg |\mu|$], the system in the ground state would be determined by the parameter Λ with $v^2/2 \sim \sqrt{f_2}\Lambda|\mu|$. However, if the sexto-linear term acts, for large Λ, as a correction to the

SM terms, the system is primarily governed by μ^2 and λ, as in the standard model. For the large-Λ expansion:

$$v^2 = v_0^2 - \frac{f_2 v_0^2}{4\lambda\Lambda^2} \qquad (A8)$$

with $v_0^2 = |\mu^2|/\lambda$.

(2) $\mu^2<0$, $\lambda>0$, $f_2<0$. In this case the Higgs potential generates a minimum away from zero and breaking the symmetry, but in addition a maximum, for large Λ far away from the minimum. The expansion in Λ,

$$\frac{v^2}{2} \approx \frac{\lambda\Lambda^2}{|f_2|}\left[\pm\left(1 - \frac{|f_2\mu^2|}{2\lambda^2\Lambda^2} - \frac{1}{8}\left(\frac{f_2\mu^2}{\lambda^2\Lambda^2}\right)^2\right) + 1\right], \quad (A9)$$
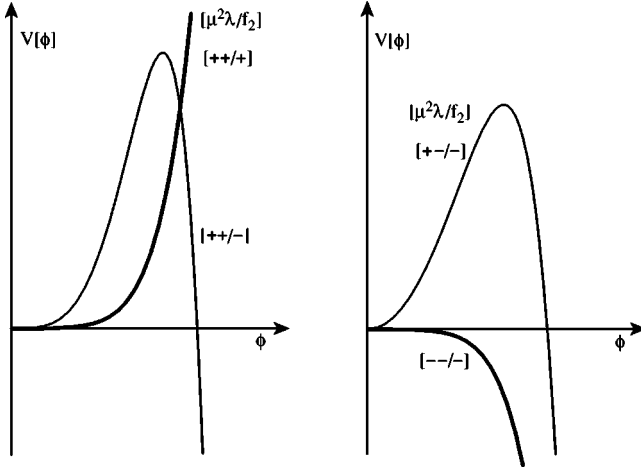
FIG. 8. Higgs potential for the four no-electroweak symmetry breaking cases. The signs of the parameters $[\mu^2, \lambda, f_2]$ are given explicitly.

the two solutions for the *loci* of the extrema are given by the values

$$v_1^2 \approx v_0^2\left(1 + \frac{|f_2|v_0^2}{4\lambda\Lambda^2}\right), \quad v_2^2 \approx v_0^2\left(\frac{4\lambda\Lambda^2}{|f_2|v_0^2} - 1\right) \approx \frac{4\lambda\Lambda^2}{|f_2|}.$$
(A10)

Clearly, the first solution v_1 is of the SM form with an order v_0^2/Λ^2 correction, and it is a deeper minimum.

The second solution v_2, however, is a maximum. If the coefficient f_2 is negative, then the potential is not bounded from below and it leads to an ultimately unstable configuration at large $|\Phi|$ [17]. In fact, if V_{eff} in Eq. (A5) holds for very large Φ [i.e., $\Phi \sim O(100\Lambda)$] then the tunneling rate to the unbounded vacuum is extremely large. However, for such large Φ the effective theory will no longer be valid and
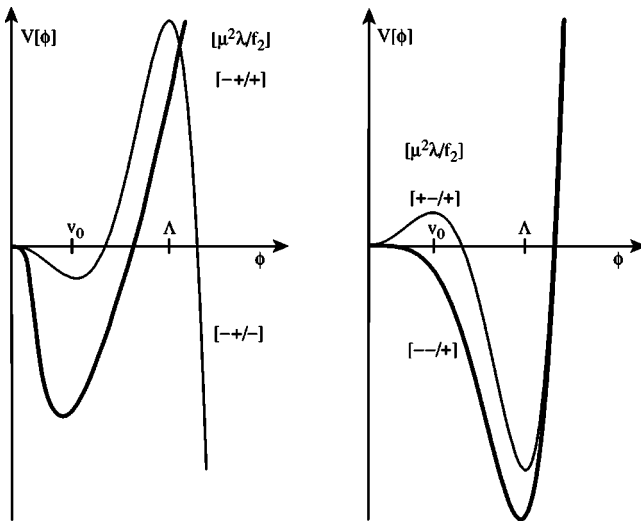

FIG. 9. Higgs potential for the four cases with symmetry breaking minima. The signs of the parameters $[\mu^2, \lambda, f_2]$ are given explicitly. The two cases in the left diagram connect smoothly to the standard model for $f_2 \rightarrow 0$.

higher-dimensional terms such as Φ^8/Λ^4 in the $1/\Lambda^2$ series will become important, so that the stability of the system can be restored again.

The instability of the system can easily be proved. If Eq. (A5) holds up to very large Φ, the tunneling rate is in the "thick-wall" regime, which can be estimated by the methods described in [33]. We sketch the calculation for the simplified case $\mu^2 = 0$, since the barrier height and width are mainly controlled by λ and f_2/Λ^2, and the shift in μ is inessential. In that case, the potential is

$$V(H) = \frac{\lambda}{4}H^4 - \frac{\kappa^2}{6}H^6,$$
(A11)

where $\Phi = H/\sqrt{2}$ and $\kappa^2 = -f_2/4\Lambda^2$. The tunneling is described by the minimum action $O(4)$ symmetric solution characterized by $r = \sqrt{\vec{x}^2 + t^2}$ for the equation of motion for H in Euclidean space. It is convenient to introduce dimensionless variables ψ and R by

$$H = \sqrt{\frac{3\lambda}{2}}\frac{\psi}{\kappa}, \quad r = \sqrt{\frac{2}{3}}\frac{\kappa R}{\lambda}.$$
(A12)

Then the tunneling rate per unit volume is proportional to $\exp(-S)$, with the minimum action configuration $S(\phi)$ given by $S(\phi) = S(\psi)/\lambda$, where

$$S(\psi) = 2\pi^2 \int_0^\infty R^3 dR\left[\frac{1}{2}\left(\frac{d\psi}{dR}\right)^2 + \frac{1}{4}\psi^4(1 - \psi^2)\right]$$
(A13)

and ψ is the solution to

$$\frac{d^2\psi}{dR^2} + \frac{3}{R}\frac{d\psi}{dR} = \psi^3\left(1 - \frac{3}{2}\psi^2\right),$$
(A14)

subject to the boundary conditions $\psi'(0) = 0$, and $\psi(\infty) = 0$. $S(\phi)$ is independent of κ, due to a compensation between the energy density in the bubble and its size. A numerical solution yields the extremely small action $S \sim 0.00084/\lambda$, which is much smaller than the value $S \gtrsim 400$ [34] needed to ensure less than one transition during the age of the observable universe. The essentially instantaneous decay is due to the extremely steep fall off of the potential for large ψ. However, as noted above, the solution is only valid if Eq. (A5) is valid up to $\psi \gtrsim \psi(0) \sim 137$, corresponding to $\phi/\Lambda \sim 335\sqrt{\lambda/|f_2|}$. The negative sign $f_2 < 0$ can therefore only be allowed, if the potential Eq. (A5) is replaced by a more complete expression before H reaches that large a value.

(3) $\mu^2 > 0$, $\lambda < 0$, $f_2 > 0$. In this case, there are three extrema that can be readily read off from Eq. (A6) for large Λ:

$$v_1^2 = 0, \quad v_2^2 \approx v_0^2\left(1 + \frac{f_2 v_0^2}{4|\lambda|\Lambda^2}\right),$$

$$v_3^2 \approx v_0^2 \left(\frac{4|\lambda|\Lambda^2}{f_2 v_0^2} - 1 \right) \approx \frac{4|\lambda|\Lambda^2}{f_2}.$$

(A15)

It turns out that following the symmetric minimum at $v_1 = 0$, there is a maximum at v_2, and there is a minimum at v_3, either above or below $V=0$. This scenario is undesirable from a theoretical point of view in any case. The reason is that the feasible vacuum v_3 is determined by $|\lambda|\Lambda^2/f_2$, and if we consider the dim-6 operators as corrections to the SM potential, we wish the vacuum not to be determined by the correction term or by the cutoff scale Λ, but rather to recover the SM by taking the decoupling limit $\Lambda \to \infty$, which would not be achieved if we accept this vacuum.

(4) $\mu^2 < 0$, $\lambda < 0$, $f_2 > 0$. In this case, following the symmetric maximum at $|\Phi| = 0$, the vacuum solution is realized for large Λ:

$$v^2 \approx v_0^2 \left(\frac{4|\lambda|\Lambda^2}{f_2 v_0^2} + 1 \right) \approx \frac{4|\lambda|\Lambda^2}{f_2}.$$

(A16)

Again, as discussed above, the solution is determined by the cutoff scale Λ, and would not be desirable to pursue.

3. Corrections to Higgs boson couplings

We first note that the dim-6 operator $\mathcal{O}_1$ corrects the kinetic terms of the Higgs boson propagation, as seen from Eq. (A3), and the full kinetic terms become

$$\mathcal{L}_{kin} = \frac{1}{2} \partial_\mu \phi \partial^\mu \phi + \frac{1}{2} \frac{f_2 v^2}{\Lambda^2} \partial_\mu \phi \partial^\mu \phi.$$

(A17)

We thus re-scale the field ϕ to define canonically normalized Higgs field H

$$\phi = NH, \quad \text{with} \quad N = (1 + a_1)^{-1/2},$$

(A18)

with $a_1 = f_1 v^2 / \Lambda^2$ used hereafter.

With this field redefinition, we find from the effective potential of Eq. (A5) the physical Higgs boson mass

$$m_H^2 = N^2 \left(\mu^2 + 3\lambda v^2 + \frac{5 f_2 v^4}{4\Lambda^2} \right)$$

$$\approx 2\lambda v^2 \left(1 - \frac{f_1 v^2}{\Lambda^2} + \frac{f_2 v^2}{2\lambda \Lambda^2} \right).$$

(A19)

As for the gauge-boson-Higgs couplings, each Higgs field receives a correction factor $N \approx 1 - a_1/2$, leading to the interactions with the linearized anomalous coupling

$$\mathcal{L}_M = \left(M_W^2 W_\mu^+ W^{-\mu} + \frac{1}{2} M_Z^2 Z_\mu Z^\mu \right) \left(N \frac{2H}{v} + N^2 \frac{H^2}{v^2} \right)$$

(A20)

$$\approx \left(M_W^2 W_\mu^+ W^{-\mu} + \frac{1}{2} M_Z^2 Z_\mu Z^\mu \right) \left(\left(1 - \frac{a_1}{2} \right) \frac{2H}{v} \right.$$

$$\left. + (1 - a_1) \frac{H^2}{v^2} \right).$$

(A21)

The Higgs self-interactions are from V_{SM}, Eqs. (A3) and (A4), and we write them in terms of the three-point and four-point couplings

$$\mathcal{L}_{H^3} + \mathcal{L}_{H^4} = -\lambda v N^3 \left(H^3 - \frac{a_1 H}{\lambda} \frac{\partial_\mu H \partial^\mu H}{v^2} + \frac{5 a_2}{6\lambda} H^3 \right)$$

$$- \frac{\lambda}{4} N^4 \left(H^4 - \frac{2 a_1 H^2}{\lambda} \frac{\partial_\mu H \partial^\mu H}{v^2} + \frac{5 a_2}{2\lambda} H^4 \right)$$

$$\approx - \frac{m_H^2}{2v} \left(\left(1 - \frac{a_1}{2} + \frac{2 a_2}{3} \frac{v^2}{m_H^2} \right) H^3 \right.$$

$$\left. - \frac{2 a_1 H \partial_\mu H \partial^\mu H}{m_H^2} \right)$$

$$- \frac{m_H^2}{8v^2} \left(\left(1 - a_1 + \frac{4 a_2 v^2}{m_H^2} \right) H^4 \right.$$

$$\left. - \frac{4 a_1 H^2 \partial_\mu H \partial^\mu H}{m_H^2} \right).$$

(A22)

The Feynman rules for the Higgs self-coupling vertices are given as

$$HHH: -i \frac{3 m_H^2}{v} \left(\left(1 - \frac{a_1}{2} + \frac{2 a_2}{3} \frac{v^2}{m_H^2} \right) + \frac{2 a_1}{3 m_H^2} \sum_{j<k}^3 p_j \cdot p_k \right)$$

(A23)

$$HHHH: -i \frac{3 m_H^2}{v^2} \left(\left(1 - a_1 + \frac{4 a_2 v^2}{m_H^2} \right) + \frac{2 a_1}{3 m_H^2} \sum_{j<k}^4 p_j \cdot p_k \right).$$

(A24)

---

[1] M. Carena, D.W. Gerdes, H.E. Haber, A.S. Turcot, and P.M. Zerwas, in Proceedings, APS/DPF/ DBP Summer Study on the Future of Particle Physics, Snowmass, 2001, hep-ph/0203229.

[2] W. Buchmüller and D. Wyler, Nucl. Phys. **B268**, 621 (1986); C.N. Leung, S.T. Love, and S. Rao, Z. Phys. C **31**, 433 (1986).

[3] J. Wudka, Int. J. Mod. Phys. A **9**, 2301 (1994).

[4] K. Hagiwara, S. Ishihara, R. Szalapski, and D. Zeppenfeld, Phys. Lett. B **283**, 353 (1992); Phys. Rev. D **48**, 2182 (1993).

[5] See the electroweak review (by J. Erler and P. Langacker) in Particle Data Group, K. Hagiwara *et al.*, Phys. Rev. D **66**, 010001 (2002).

[6] G.J. Gounaris, D.T. Papadamou, and F.M. Renard, Z. Phys. C **76**, 333 (1997).

[7] M. Beneke *et al.*, hep-ph/0003033; F. Larios, E. Malkawi, and C.-P. Yuan, hep-ph/9704288.

[8] Z.H. Lin, T. Han, T. Huang, J.X. Wang, and X. Zhang, Phys. Rev. D **65**, 014008 (2002).

[9] T. Han, T. Huang, Z.H. Lin, J.X. Wang, and X. Zhang, Phys. Rev. D **61**, 015006 (2000).

[10] TESLA: Technical Design Report (Part 3), edited by R.D. Heuer, D.J. Miller, F. Richard, and P.M. Zerwas, DESY 010-011, hep-ph/0106315.

[11] American LC Working Group, T. Abe *et al.*, SLAC-R-570, 2001, hep-ex/0106055-58; ACFA LC Working Group, K. Abe *et al.*, KEK-REPORT-2001-11, hep-ex/0109166.

[12] CLIC Study Team, R.W. Assmann *et al.*, CERN-2000-008.

[13] F. Boudjema and E. Chopin, Z. Phys. C **73**, 85 (1996).

[14] P.M.Z. thanks L. Maiani for discussions on this effective potential.

[15] For a recent review, see, e.g., C. Hill and E. Simmons, hep-ph/0203079.

[16] R. Casalbuoni and L. Marconi, hep-ph/0207280.

[17] A. Datta, B.L. Young, and X. Zhang, Phys. Lett. B **385**, 225 (1996); B. Grzadkowski and J. Wudka, Phys. Rev. Lett. **88**, 041802 (2002); C.P. Burgess, V. Di Clemente, and J.R. Espinosa, J. High Energy Phys. **01**, 041 (2002).

[18] K. Desch and N. Meyer, prepared for 5th International Linear Collider Workshop (LCWS 2000), Fermilab, Batavia, Illinois, 2000, LC-PHSM-2001-025.

[19] C. Castanier, P. Gay, P. Lutz, and J. Orloff, hep-ex/0101028.

[20] M. Battaglia, E. Boos, and W.-M. Yao, hep-ph/0111276.

[21] J.F. Gunion, T. Han, and R. Sobey, Phys. Lett. B **429**, 79 (1998).

[22] W. Kilian, M. Krämer, and P. Zerwas, Phys. Lett. B **381**, 243 (1996); G.J. Gounaris, F.M. Renard, and N.D. Vlachos, Nucl. Phys. **B459**, 51 (1996).

[23] A. Pukhov *et al.*, INP-MSU-98-41-542, hep-ph/9908288.

[24] M. Meyer and K. Desch, talk at the ECFA/DESY Linear Collider Workshop, St. Malo, France, 2002.

[25] G.J. Gounaris, D. Schildknecht, and F.M. Renard, Phys. Lett. **83B**, 191 (1979); V. Barger and T. Han, Mod. Phys. Lett. A **5**, 667 (1990); V.A. Ilyin, A.E. Pukhov, Y. Kurihara, Y. Shimizu, and T. Kaneko, Phys. Rev. D **54**, 6717 (1996).

[26] A. Djouadi, H.E. Haber, and P.M. Zerwas, Phys. Lett. B **375**, 203 (1996); A. Djouadi, W. Kilian, M. Muhlleitner, and P.M. Zerwas, Eur. Phys. J. C **10**, 27 (1999); P. Osland and P.N. Pandita, Phys. Rev. D **59**, 055013 (1999); F. Boudjema and A. Semenov, *ibid.* **66**, 095007 (2002).

[27] D.J. Miller and S. Moretti, Eur. Phys. J. C **13**, 459 (2000).

[28] Y. Yasui *et al.*, hep-ph/0211047.

[29] S. Kanemura *et al.*, Phys. Lett. B **558**, 157 (2003).

[30] M. Battaglia, talk at the International Linear Collider Conference LCWS2002, Jeju Island, Korea, 2002.

[31] For a recent discussion on CLIC parameters and physics goals, see, e.g., T. Barklow and A. De Roeck, hep-ph/0112313.

[32] D. Rainwater, T. Plehn, and U. Baur, Phys. Rev. Lett. **89**, 151801 (2002); U. Baur, T. Plehn, and D. Rainwater, Phys. Rev. D **67**, 033003 (2003); F. Gianotti *et al.*, hep-ph/0204087.

[33] A.D. Linde, Nucl. Phys. **B216**, 421 (1983); **B223**, 544(F) (1983).

[34] A. Kusenko, P. Langacker, and G. Segre, Phys. Rev. D **54**, 5824 (1996).